SUPPLEMENTAL DATA

Online Tables

Table S1. Primer sequences used for RT-PCR.

Gene		Sequences (5'→3')
Mhy6	for	CGGGAGAACCAGTCCATCCT
	rev	ACACGCTTCGTGTTGACAGTCT
	probe	SYBR
Mhy7	for	GCCAAGACAGTTCGGAATGATAA
	rev	CCTGTTGCCCCAAAATGG
	probe	SYBR
Fn	for	GGACCTGCACGCCAATAGCT
	rev	TCCCCCACGACGTAGGAA
	probe	AGAAATGTTTTGATCACGCTGCTGGGA
Ctgf	for	CGCCAACCGCAAGATTG
	rev	CACGGACCCACCGAAGAC
	probe	CACTGCCAAAGATGGTGCACCCTG
Ngal	for	CAGGGCAGGTGGTTCGTT
	rev	AGCGGCTTTGTCTTTCTTTCTG
	probe	TCGGCCTGGCAGCGAATGC
18S	for	ACATCCAAGGAAGGCAGCAG
	rev	TTTTCGTCACTACCTCCCCG
	probe	CGCGCAAATTACCCACTCCCGAC
Nfkbia	for	CCTGTACGCCCCAGCATCT
	rev	TAGACACGTGTGGCCGTTGT
	probe	SYBR
Kcnj3	for	TGCGCAACAGCCACATG
	rev	AGGTGTCTGCCGAGATTTGAG
	probe	SYBR
Timp4	for	TGCTGGAACGGAAGCTCTATG
	rev	GCAGATGCCATCAACATGCT
	probe	SYBR
Mmp15	for	CACCCATTTCGACGCAGAT
	rev	CATGCACAGCCACCAGAAAG
	probe	SYBR
Pparg	for	TGACTTGGCCATATTTATAGCTGTCA
	rev	CGATGGGCTTCACGTTCAG
	probe	SYBR

Cx3cl1	for	GCAAGCGCGCCATCA
	rev	TGGACCCATTTCTCCTTTGG
	probe	SYBR
Myc	for	CGAGCTGAAGCGTAGCTTTTTT
	rev	GGCCTTTTCGTTGTTTTCCA
	probe	SYBR
Mt1a	for	CGGCTGCAAGAACTGCAAAT
	rev	ACTTGTCCGAGGCACCTTTG
	probe	SYBR
Hmox1	for	GGCCTGGCTTTTTTCACCTT
	rev	CGAGCACGATAGAGCTGTTTGA
	probe	SYBR
Kcnd2	for	GCAGAGCAAGCGGAATGG
	rev	GCTAACGAAGGCCGGTTCA
	probe	SYBR
Trpv4	for	CCTATCTGTGTGCCATGGTCAT
	rev	TCCACTGTGGTCCGGTAAGG
	probe	SYBR
Scn4b	for	GCCACCACCATCTACGCTATC
	rev	AGCCATAACAGCTGGAGAAGGT
	probe	SYBR

Online Figures

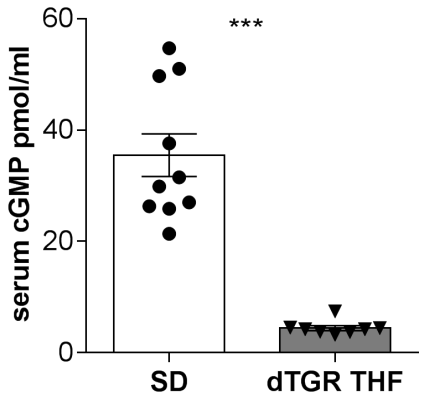

Figure S1. dTGRs with terminal heart failure (THF) exhibit significantly reduced serum cGMP levels compared to SD control rats (***p<0.001; Mann-Whitney U test; data expressed as mean±SEM; SD n=10; dTGR THF n=8).

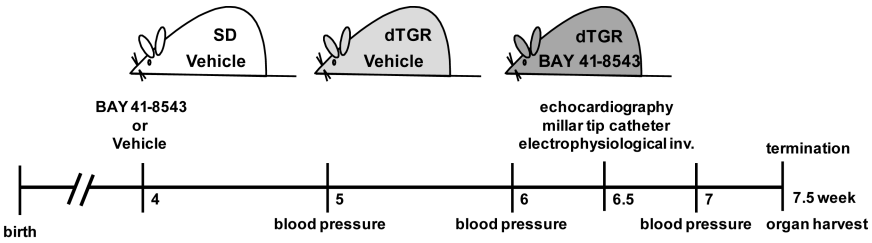

Figure S2. Experimental flow chart of *in vivo* study design.

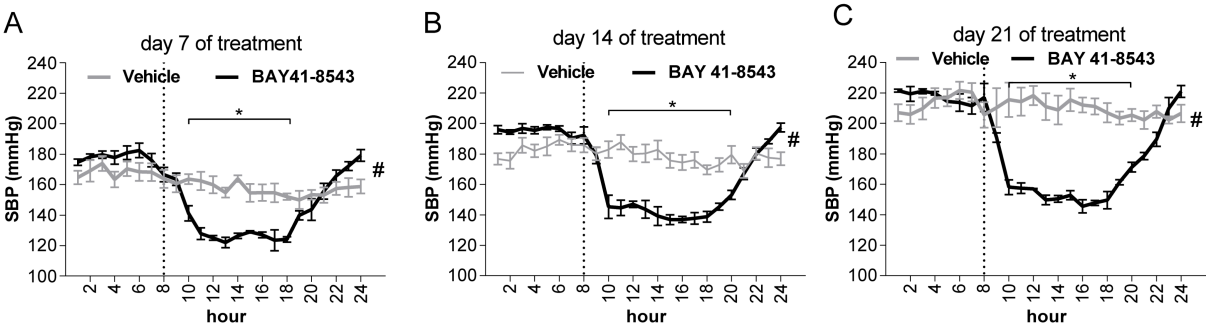

Figure S3. 24-hour time course of telemetrically recorded systolic blood pressure (SBP) on day 7 (A), 14 (B) and 21 (C) in vehicle (n=5) and BAY 41-8543-treated dTGR (n=4). Dotted line represents oral gavage of vehicle or BAY 41-8543. ($^{\#}$ p<0.5 Two-way ANOVA; data expressed as mean±SEM)

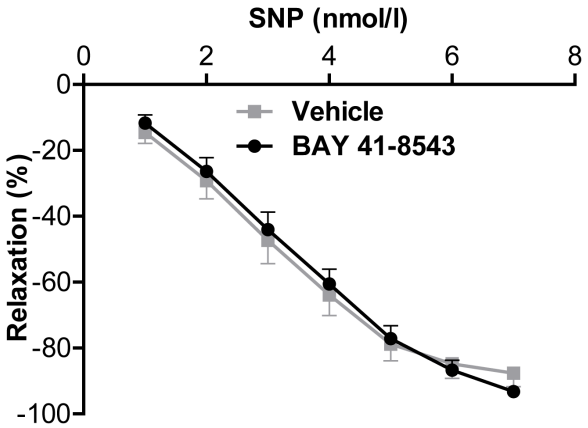

Figure S4. Endothelial independent relaxation of mesenteric arteries by sodium nitroprusside was similar in BAY 41-8543-treated compared to vehicle-treated dTGR. (data expressed as mean±SEM; Vehicle n=27; BAY 41-8543 n=29)

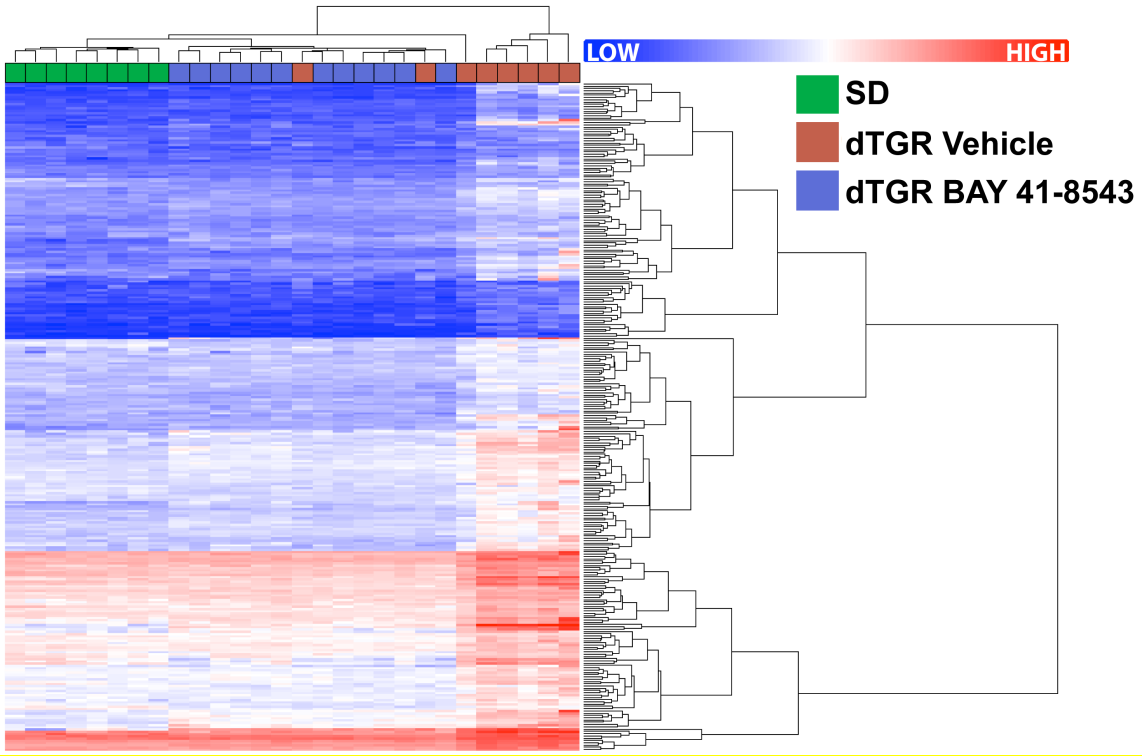

Figure S5. Two-way hierarchical clustering of the 844 genes whose expression significantly changed between BAY 41-8543 and vehicle-treated dTGR. The mRNA clustering tree is shown on the right and the sample clustering tree appears at the top (green circles for SD rats, red diamonds for vehicle treated dTGR and blue squares for BAY 41-8543 treated dTGR). The color scale indicates the relative expression level of mRNAs, with red representing a high expression level and blue a low expression level. (SD n=8; Vehicle n=8; BAY 41-8543 n=12)

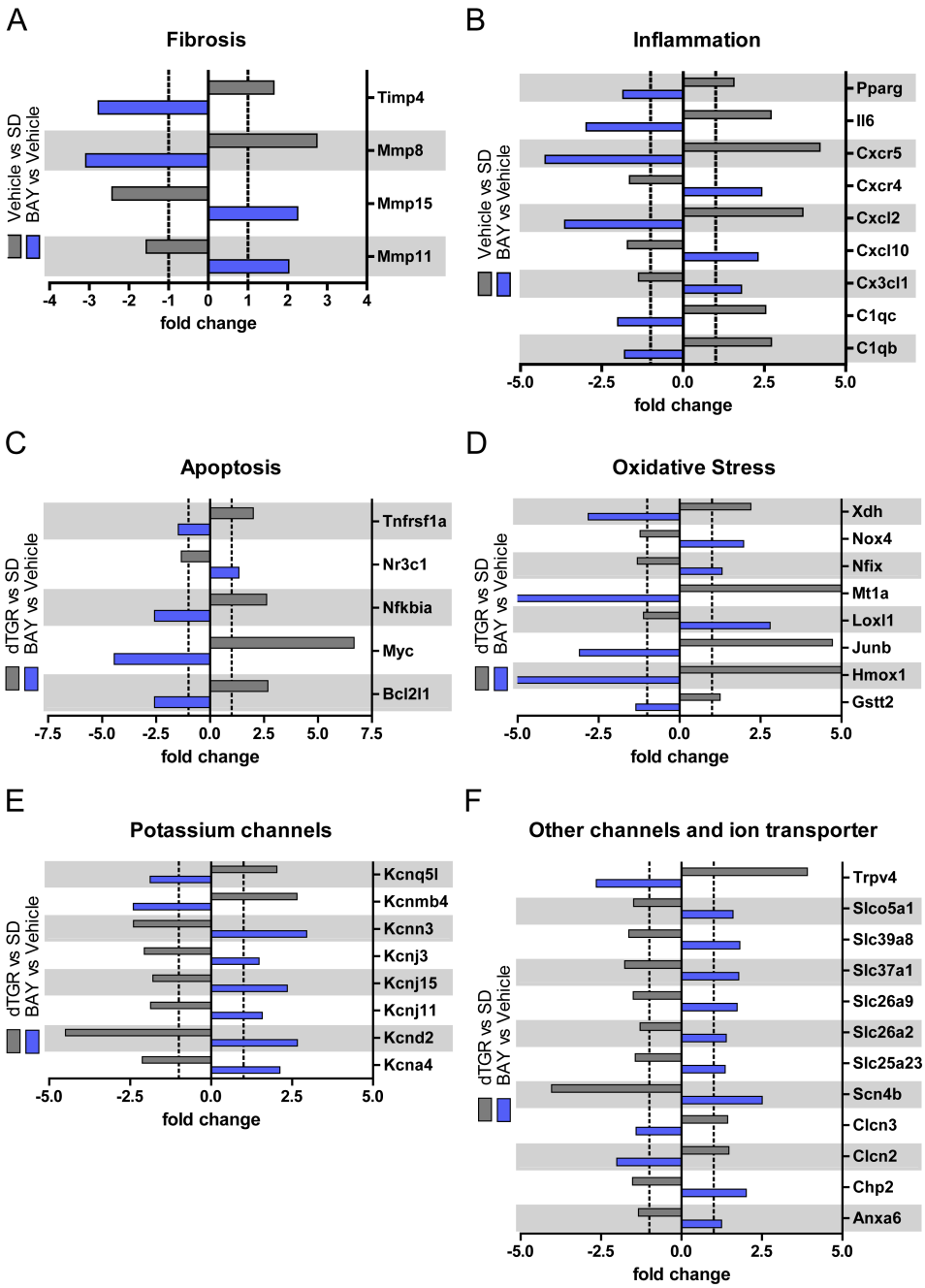

Figure S6. GO term functional analysis showed amelioration of dysregulated genes in the heart of dTGR by BAY 41-8543 treatment had an impact on fibrosis inflammation, apoptosis, oxidative stress, potassium channels and other channels and ion transporters.

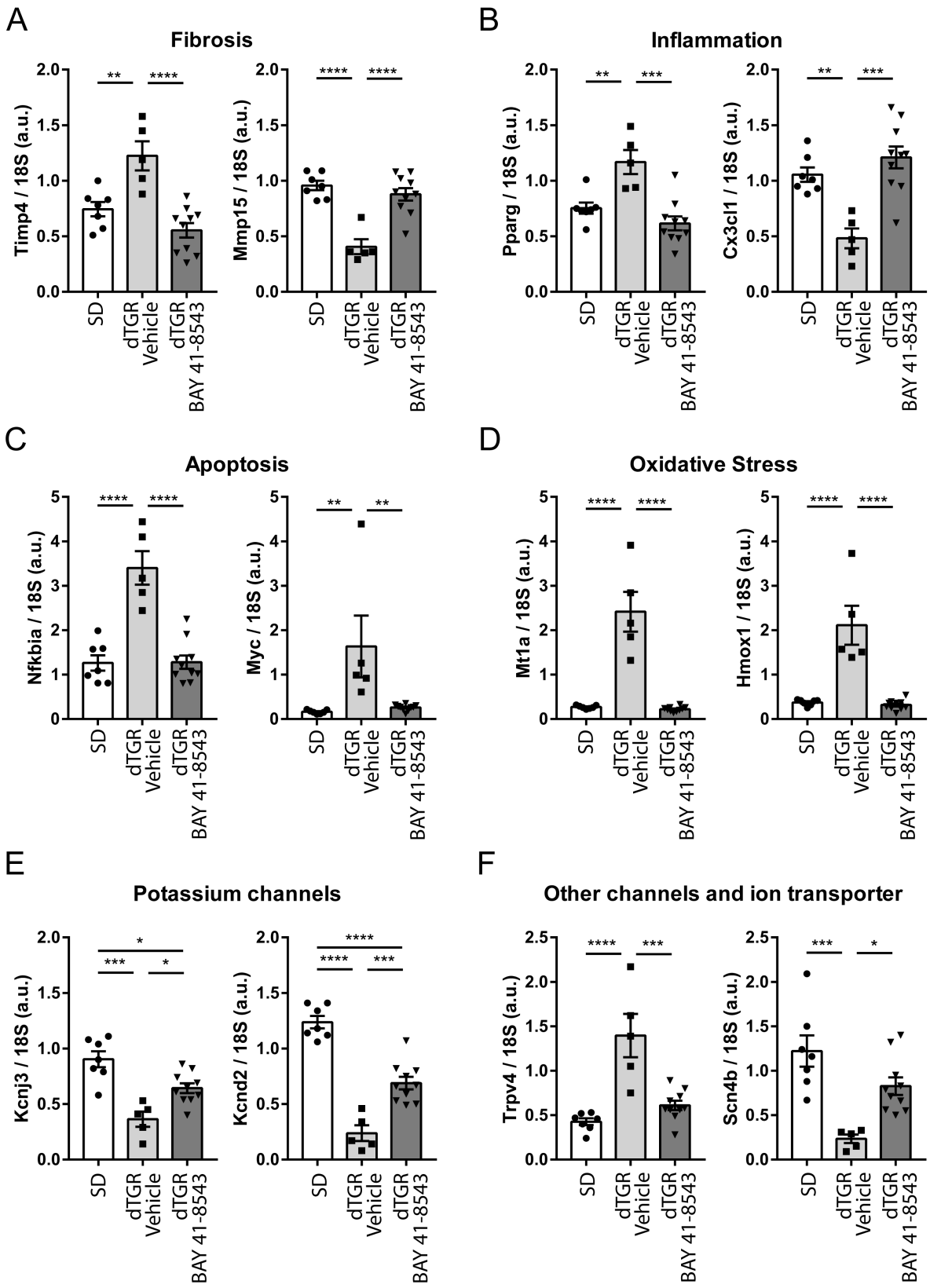

Figure S7. A) Cardiac mRNA expression of the fibrosis-related genes metalloproteinase inhibitor 4 (Timp4) and matrix metalloproteinase 15 (Mmp15). **B)** Cardiac mRNA expression of the inflammation-related genes peroxisome proliferator-

activated receptor gamma (Pparg) and fractalkine (Cx3cl1). **C)** Cardiac mRNA expression of the apoptosis-related genes nuclear factor 'kappa-light-chain-enhancer' of activated B-cells inhibitor alpha (Nfkbia) and Myc. **D)** Cardiac mRNA expression of the oxidative stress-related genes metallothionein-1A (Mt1a) and heme oxygenase 1 (Hmox1). **E)** Cardiac mRNA expression of the potassium inwardly-rectifying channel subfamily J member 3 (Kcnj3) and potassium voltage-gated channel subfamily D member 2 (Kcnd2). **F)** Cardiac mRNA expression of the transient receptor potential cation channel subfamily V member 4 (Trpv4) and sodium channel β-subunit 4 (Scn4b).

(*p<0.05, **p<0.01, ***p<0.001, ****p<0.0001; one-way ANOVA with Tukey's post hoc test; data expressed as mean±SEM; (SD n=7; Vehicle n=5; BAY 41-8543 n=10).

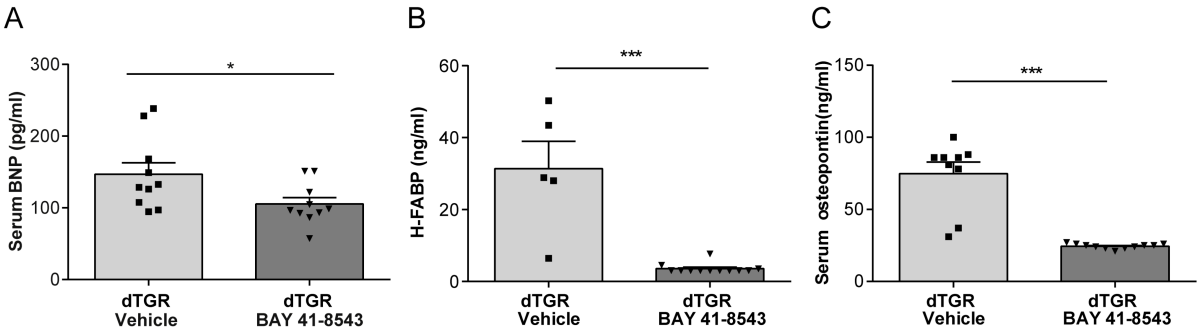

Figure S8. Serum BNP (A), H-FABP (B) and Osteopontin (C) levels were significantly decreased in BAY 41-8543-treated dTGR compared to vehicle-treated dTGR. (*p<0.05 ***p<0.001; Student t-test test; data expressed as mean±SEM; Vehicle n=5-10; BAY 41-8543 n=10-11)

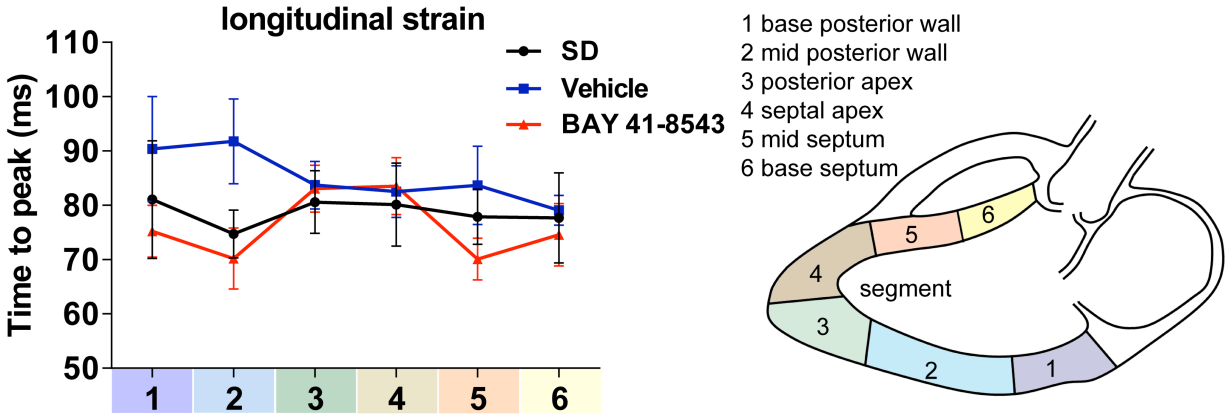

Figure S9. Time to peak longitudinal strain showed no changes in vehicle-treated dTGRs compared to nontransgenic SD rats and BAY 41-8543 treated dTGRs within the six myocardial segments. (Two-way ANOVA; data expressed as mean ± SEM; SD n=4; Vehicle n=6; BAY 41-8543 n=10) Left ventricle was divided into six segments in parasternal long axis.

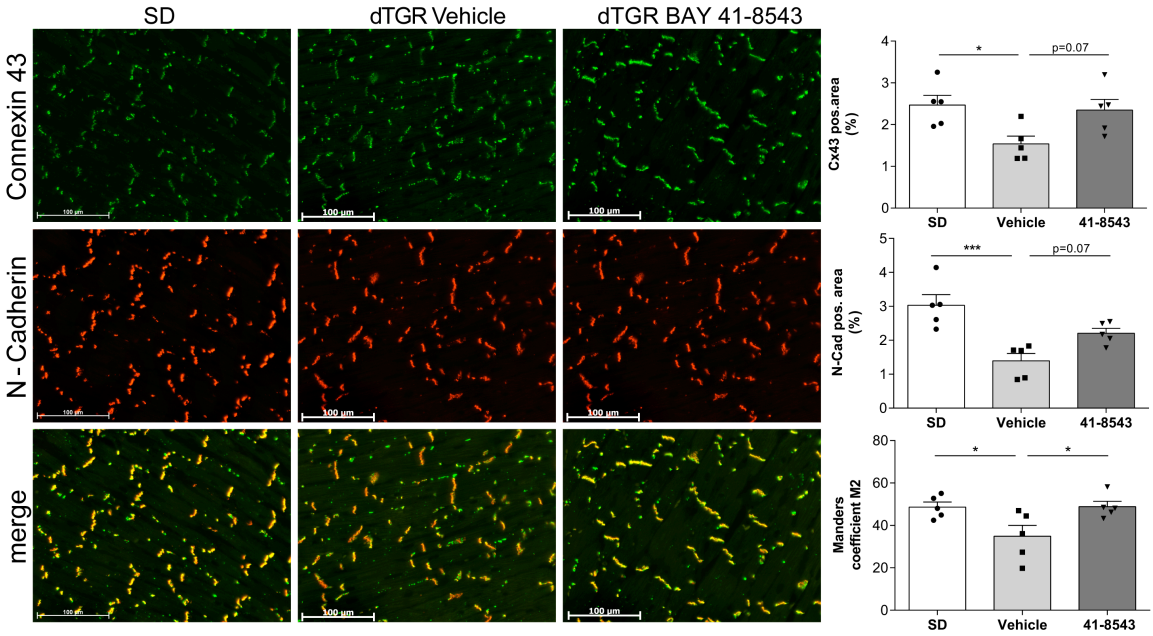

Figure S10. Representative immunofluorescence stainings of left ventricular sections prepared from SD rats, vehicle-treated and BAY 41-8543-treated dTGR. The sections were co-stained for connexin 43 (Cx43) (green fluorescent signal) and N-cadherin (N-Cad) (red). Cx43 and N-cad are colocalized (yellow) to the intercalated disks. This normal Cx43 localization was largely preserved in BAY 41-8543-treated dTGR,

whereas in vehicle-treated dTGR a redistribution of Cx43 could be observed. Quantitative analysis of Cx43, N-cadherin and colocalization of Cx43 and N-cadherin was performed and is shown on the right side. (*$p<0.05$; one-way ANOVA with Tukey's post hoc test; data expressed as mean±SEM; SD n=5; Vehicle n=5; BAY 41-8543 n=5)